

Complex Formation between Cationic Polymethacrylates and Oligonucleotides

E. Van Rompaey, N. Sanders, S. C. De Smedt,* and J. Demeester

Laboratory of General Biochemistry and Physical Pharmacy, Ghent University, Harelbekestraat 72, 9000 Ghent, Belgium

E. Van Craenenbroeck and Y. Engelborghs

Laboratory of Biomolecular Dynamics, University of Leuven, Celestijnenlaan 200D, 3001 Leuven, Belgium

Received May 22, 2000; Revised Manuscript Received August 16, 2000

ABSTRACT: With regard to the development of pharmaceutical carriers for oligonucleotides, the interactions between a cationic polymer, poly(2-dimethylamino)ethyl methacrylate (pDMAEMA), and rhodamine-labeled 25-mer phosphodiester oligonucleotides (Rh-ONs) were studied. The composition of the pDMAEMA/Rh-ON complexes was investigated as a function of the charge ratio (φ ; +/-) by increasing the pDMAEMA concentration and keeping the Rh-ON concentration constant. Gel electrophoresis revealed that at $\varphi < 1$ only a fraction of the short Rh-ONs bind the longer pDMAEMA chains. Dynamic light scattering and zeta potential (ζ) indicated that at $\varphi < 1$ only a fraction of the phosphate anions on the Rh-ONs are involved in complex formation which results in “dangling” of the Rh-ONs. Moreover, from fluorescence measurements, multimolecular complexes (i.e., several Rh-ONs per pDMAEMA chain) were revealed. At $1 < \varphi < 3$, ζ approximated zero. This led to a clustering of individual complexes. At $\varphi > 3$, all the Rh-ONs were bound while, compared to complexes at $\varphi < 1$, the average number of Rh-ONs bound to one pDMAEMA chain was decreased. The presence of multimolecular complexes was confirmed from fluorescence correlation spectroscopy (FCS) measurements. The multimolecular complexes were observed as highly intense fluorescent particles upon their diffusion through the confocal volume of the FCS instrument. Also, the decrease in the average number of Rh-ONs bound to one pDMAEMA chain, upon increasing φ , was confirmed by FCS.

Introduction

The use of oligonucleotides (ONs) to down regulate the production of specific gene products requires the entry of ONs into the cytoplasm and/or nucleus of the cells, to be able to hybridize with their targets. Entry into the nucleus is required when considering triple-helix therapy, where the ONs form triple-stranded helices with DNA and consequently inhibit transcription. When the antisense approach is considered, which aims to bind the ONs to natural sense mRNA in order to inhibit translation, the hybridization can take place in the cytoplasm as well as in the nucleus. Generally, the cellular uptake of ONs is very poor due to their large size, hydrophilicity, and negatively charged backbone. Furthermore, especially unmodified phosphodiester ONs are very susceptible to nuclease activity.¹ To bypass these problems, cationic lipids and cationic polymers, which spontaneously form soluble interpolyelectrolyte complexes with the negatively charged nucleic acids (called lipoplexes and polyplexes,² respectively), are under investigation as pharmaceutical carriers for ONs.^{3–6}

The physicochemical and biological features that govern the activity of ON delivery systems are not very well understood. Despite major efforts to understand the physicochemical behavior of interpolyelectrolyte complexes, the mechanism of complex formation between polycations and nucleic acids is still unknown due to the high complexity of the phenomena. Nevertheless,

the association to and dissociation of ONs from such carriers are critically important both in vitro and in vivo. If the affinity between the ONs and the cationic carriers is too low, the complex will dissociate prematurely, e.g., in the bloodstream, while a strong affinity might prevent the release of the ONs intracellularly, a necessity to allow interaction with their target.

Many methods exist to study the association and dissociation of ONs and plasmids to/from their carrier in nonbiological environments. Often applied for this purpose are gel electrophoresis, fluorescence-based assays such as fluorescence resonance energy transfer (FRET), and density gradient analysis.^{7,8} Very recently, electron paramagnetic resonance⁹ and surface plasmon resonance spectrometry¹⁰ were introduced to investigate the interactions between nucleic acids and polycations.

However, to obtain real breakthroughs in the design and the understanding of the dissociation of polyplexes in biological environments such as cells, there is an urgent need for advanced physicochemical methods, which allow us to characterize these critical steps not only in vitro but also in biological media.

In the present paper, we aimed to understand the complex formation between rhodamine-labeled ONs and poly(2-dimethylamino)ethyl methacrylate (pDMAEMA, Figure 1), a cationic polymer, which is currently under investigation as a pharmaceutical carrier for nucleic acids.^{11–15} Moreover, we have introduced fluorescence correlation spectroscopy (FCS), a technique which shows potential to be applied on a cellular scale, as a novel tool for studying the interactions between cationic polymers and ONs. Basically, as illustrated in Figure

* Corresponding author. Telephone 32-9-264 80 76; fax 32-9-264 81 89; e-mail stefaan.desmedt@rug.ac.be.

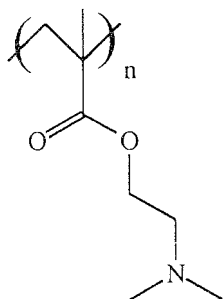


Figure 1. 2-(Dimethylamino)ethyl methacrylate, being the monomer of pDMAEMA. The pK_a of the amine equals 7.5.

2, FCS monitors the fluorescence fluctuations caused by the diffusion of fluorescently labeled ONs through the confocal volume of a microscope. Upon binding to large cationic polymers, which are themselves not excitable by the laser light, one can expect that the diffusion of the Rh-ONs slows down, which may consequently influence the fluorescence fluctuations.¹⁶

Experimental Section

Oligonucleotides. The 25-mer phosphodiester ONs (5'-TCT-GGG-TCA-TCT-TTT-CAC-GGT-TGG-C-3') and 25-mer rhodamine labeled phosphodiester ONs were purchased from Eurogentec. The fluorescent labeling occurred at the 5' end of the ONs: each Rh-ON molecule contained one Rh label. The concentration of the ON and Rh-ON stock solutions (in Tris-buffer at pH 8) was determined by measuring the absorption at 260 nm ($1 \text{ OD}_{260} = 33 \mu\text{g ON/mL}$) and equaled 64 and 46 $\mu\text{g/mL}$, for the ON and Rh-ON stock solution, respectively. The molecular mass of the ONs and Rh-ONs was 7646 and 8253 g/mol, respectively.

Cationic Polymers. Poly(2-dimethylamino)ethyl methacrylate, a kind gift of the University of Utrecht, was synthesized and characterized as described elsewhere.¹⁴ The molecular mass of the DMAEMA monomer equaled 157 g/mol. The number-average molecular mass (M_n) of pDMAEMA was estimated to be around 60 000 g/mol as determined by gel permeation chromatography (GPC). As no pDMAEMA molecular weight standards are available, dextran molecular weight standards were used to estimate M_n from GPC. The pK_a of the amine group in pDMAEMA equaled 7.5 and was determined by titration as described elsewhere.¹⁷

Preparation of Polyplexes. pDMAEMA/Rh-ON complexes differing in charge ratio (φ), but having the same Rh-ON concentration (10 $\mu\text{g/mL}$, 1.2 μM), were prepared. φ , being the ratio (+/-) of the positive charge equivalents of pDMAEMA to the negative charge equivalents of Rh-ON, was calculated assuming that 1 μg of 25-mer Rh-ON contains 2.91 nmol negative charges and 1 μg of pDMAEMA contains 3.54 nmol positive charges as calculated from the molecular mass of the DMAEMA monomer and the pK_a of the pDMAEMA. Two methods of preparing the pDMAEMA/Rh-ON complexes were considered in this study. In the "fast addition method", the pDMAEMA/Rh-ON complexes (varying in φ) were prepared by adding different volumes of the pDMAEMA stock solution (347 $\mu\text{g/mL}$ in 20 mM Hepes buffer at pH 7.4) to a fixed volume of the Rh-ON stock solution in one step. After addition of the polymer solution, the dispersion was vortexed for 10 s. To obtain the final Rh-ON concentration of 10 $\mu\text{g/mL}$, the dispersions were further diluted with Hepes buffer at pH 7.4. The polyplexes were allowed to equilibrate for 30 min at room temperature before use. In the "slow addition method", the complexes were prepared by adding drop by drop the pDMAEMA/Hepes mixture (with the same volume but with varying concentration of pDMAEMA to obtain polyplexes with a different charge ratio) to a fixed volume of the Rh-ON stock solution. After the addition of each drop of polymer solution, the dispersion was vortexed. The polyplexes were allowed to equilibrate for 30 min at room temperature before use. Particle

size, zeta potential, fluorescence measurements, and gel electrophoresis were all done on the same pDMAEMA/Rh-ON dispersions, having a final Rh-ONs concentration of 10 $\mu\text{g/mL}$ (1.2 μM).

For FCS measurements, the pDMAEMA/Rh-ONs dispersions were prepared by the fast addition method as described above. However, the final Rh-ONs concentrations equaled 0.025 $\mu\text{g/mL}$ (3 nM).

Particle Size Measurements. Dynamic light scattering measurements (DLS) on pDMAEMA/Rh-ON complexes were carried out on a Malvern 4700 instrument (Malvern) at 25 °C and at an angle of 90°. The incident beam was a HeNe laser beam (633 nm). The pDMAEMA/Rh-ON complexes were prepared as described above. To avoid dust particles, the pDMAEMA solutions were filtered before being added to the nucleotide solutions. Average pore size of the filter was 0.45 μm (Schleicher & Schuell). The particle size was measured 30 min after the preparation of the pDMAEMA/Rh-ON complexes. For calculating the z -average hydrodynamic diameter from the DLS data, the viscosity and refractive index of water at 25 °C (0.89 mPa·s and 1.333, respectively) were used. Polystyrene nanospheres ($220 \pm 6 \text{ nm}$, Duke Scientific Corp) were used to verify the performance of the instrument. The particle size of each dispersion (as characterized by φ) was measured three times.

Zeta Potential Measurements. Zeta potential (ζ) measurements on the pDMAEMA/ON complexes were performed at 25 °C on a Malvern Zetasizer 2000 (Malvern), which is based on electrophoretic light scattering. ζ was measured within 1 h after the preparation of the pDMAEMA/ON complexes. Polystyrene nanospheres (-50 mV , Duke Scientific Corp) were used to verify the performance of the instrument. ζ of each dispersion was measured three times.

Fluorescence Measurements. The fluorescence of pDMAEMA/Rh-ON complexes was measured 30 min after their preparation on an SLM-Aminco Bowman fluorimeter (SLM-Aminco Bowman; $\lambda_{\text{ex}} = 525 \text{ nm}$, $\lambda_{\text{em}} = 584 \text{ nm}$). Fluorescence of each dispersion was measured three times.

Gel Electrophoresis Experiments. Gel electrophoresis was performed on the same polyplex dispersions as used for particle size, ζ , and fluorescence measurements. After preparation, the dispersions were allowed to stand at room temperature for 30 min. They were diluted with loading buffer (90% dispersion + 10% loading buffer which consisted of 50% sucrose in distilled water containing bromophenol blue). A 20 μL aliquot of this mixture was placed in the wells of a 2.5% agarose gel. A TBE buffer was used containing 10.8 g/L Tris base, 5.5 g/L boric acid, and 0.58 g/L EDTA. The total concentration of oligonucleotides in the wells was 0.18 μg . A potential of 100 V was applied for 50 min. The oligonucleotides were detected by staining the gel with a SYBR Green I solution (Molecular Probes; 100 μL SYBR Green I in 1L TBE buffer adjusted to a pH between 7.5 and 8).

Fluorescence Correlation Spectroscopy (FCS). The translational mobility of Rh-ONs and polyplexes in buffer was measured using FCS, which is based on the analysis of intensity fluctuations of excited fluorescent molecules caused by diffusion through the confocal volume of a microscope (Figure 2).¹⁸ The fluorescent molecules are excited by a stationary laser beam, and the autocorrelation function of the fluctuations allows us to compute the translational diffusion time (τ_d) and the average total number of fluorescent molecules in the illuminated volume (N). The translational diffusion time is the average time a fluorescent molecule spends in the excitation volume.

Fluorescence fluctuations may arise from phenomena such as Brownian diffusion, flow, and chemical reactions. When the fluorescence fluctuations are only due to diffusion through the confocal volume, which is approximated as a cylinder with radius ω_1 and height $2\omega_2$ (Figure 1), $G(\tau)$ takes the following form:¹⁹

$$G(\tau) = 1 + \frac{1}{N} f(\tau/\tau_d) \quad (1)$$

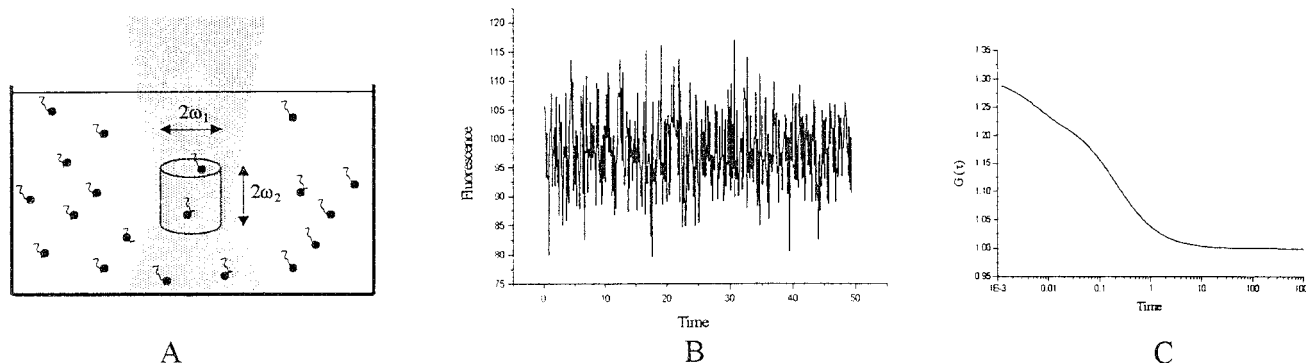


Figure 2. Passage of fluorescent molecules through the confocal volume element (A) gives rise to fluctuations in measured fluorescence (B). An autocorrelation function (C) can be derived from the fluctuations and allows to calculate the average residence time in the confocal volume.

with

$$f(\tau/\tau_d) = \left[\frac{1}{1 + \tau/\tau_d} \right] \left[\frac{1}{1 + (\omega_1/\omega_2)^2 \tau/\tau_d} \right]^{1/2} \quad (2)$$

For a mixture of two types of fluorescent molecules exhibiting a fast (τ_{free}) and a slow (τ_{bound}) translational diffusion time, $G(\tau)$ reads¹⁹

$$G(\tau) = 1 + \frac{1}{N} [(1 - y)f(\tau/\tau_{\text{free}}) + yf(\tau/\tau_{\text{bound}})] \quad (3)$$

where $(1 - y)$ and y are the molar fractions of the free and the bound component, respectively. The translational diffusion coefficient (D) is calculated from τ_d by the following equation:

$$D = \frac{\omega_1^2}{4\tau_d} \quad (4)$$

As the amplitude of the autocorrelation function is inversely proportional to the occupation number N , it allows the calculation of the concentrations of fluorescent molecules by the following equation:

$$C \text{ (mol/L)} = \frac{N}{6.02 \times 10^{23} \cdot 2\pi\omega_1^2\omega_2} \quad (5)$$

A commercial FCS instrument (Confocor, Zeiss-Evotec) was used. Briefly, the light of a HeNe laser operating at 543 nm was projected into the microscope water immersion objective (C-apochromat 40 \times magnification) via a dichroic mirror. The laser beam was focused at about 180 μm above the bottom of the cuvettes (Nalge Nunc International), which contained the Rh-ON solutions or polyplex dispersions. Laser power was adapted by inserting a neutral density filter. The emitted light was collected by the same objective and passed through the dichroic mirror and the 45 μm pinhole to finally reach the avalanche photodiode. Measurements on the Rh-ON solution were performed at room temperature on samples of 200 μL . The measuring time on the Rh-ON solution was 50 s, and the sample was measured 10 times. For FCS measurements on the pDMAEMA/Rh-ON complexes, 200 μL of the dispersions was prepared by the fast addition method in an Eppendorf tube (Eppendorf), vortexed, and immediately transferred into the FCS Nunc cuvettes to begin the FCS measurement. Each dispersion (as characterized by φ) was measured 60 times. For each measurement, the fluorescence fluctuations were recorded for 50 s.

As the size of the excited sample region (Figure 1) is affected by small variations in optical alignment, before starting the measurements, the volume element must be calibrated. ω_1 and ω_2 were determined using a rhodamine 6G solution (5 nM in water) with known diffusion coefficient ($2.8 \times 10^{-6} \text{ cm}^2/\text{s}$). FCS measurements on the rhodamine 6G solution were performed

at room temperature, using a 0.5 neutral density filter, while the fluorescence signal was autocorrelated over 25 s. τ_d of the rhodamine 6G molecules, as calculated from $G(\tau)$, equaled $72 \pm 2 \mu\text{s}$. ω_1 , as calculated from eq 4, equaled 0.28 μm . The structural parameter of the confocal volume element (ω_2/ω_1) equaled 8.17 as determined from $G(\tau)$ of the rhodamine 6G solution and allowed us to calculate ω_2 , which equaled 2.29 μm .

Results and Discussion

Size and Zeta Potential of pDMAEMA/ON Complexes. None of the pDMAEMA/Rh-ON dispersions used for size and zeta potential measurements were apparently turbid. However, despite their transparent appearance, light scattering increased upon adding pDMAEMA to the Rh-ON solutions, suggesting the formation of nanosized particles through the complexation of the Rh-ON with pDMAEMA. Figure 3 shows the hydrodynamic size and ζ of pDMAEMA/Rh-ON polyplexes as a function of φ . Both a "slow addition method" and a "fast addition method" were used to prepare the polyplexes, as it was reported previously that the way of preparation may have a substantial influence on the properties of the resulting polyplexes.²⁰ As each point originates from DLS and zeta potential measurements on three polyplex dispersions, which were independently prepared, the way we prepared the polyplexes resulted in complexes that were fairly reproducible with regard to their size and surface properties. Only at low values of φ , the way of adding the pDMAEMA solution to the Rh-ON solution seemed to have an influence on the size of the resulting polyplexes.

The dependence of the size and surface properties of the pDMAEMA/Rh-ON complexes on φ shows a typical profile as often observed for complexes formed between oppositely charged polyions.²¹ At low values of φ , nonstoichiometric polyplexes form, in which the amount of protonated amines is lower than the amount of phosphate anions and which are negatively charged. The interpretation of this is shown in Figure 4A. A fraction of the short and flexible Rh-ON chains binds only partially to the longer pDMAEMA chains which implies that only a few of the phosphate anions on the Rh-ON chains are involved in complex formation. The nonneutralized anions provide for the water solubility of the polyplexes and for their negative net charge. Another fraction of the Rh-ONs chains remains free in solution. Electrophoresis indeed confirmed that, at values of $\varphi < 1$, free Rh-ONs are present (data not shown). We wondered whether, at values of $\varphi < 1$ (Figure 3), the particle size and ζ correspond to indi-

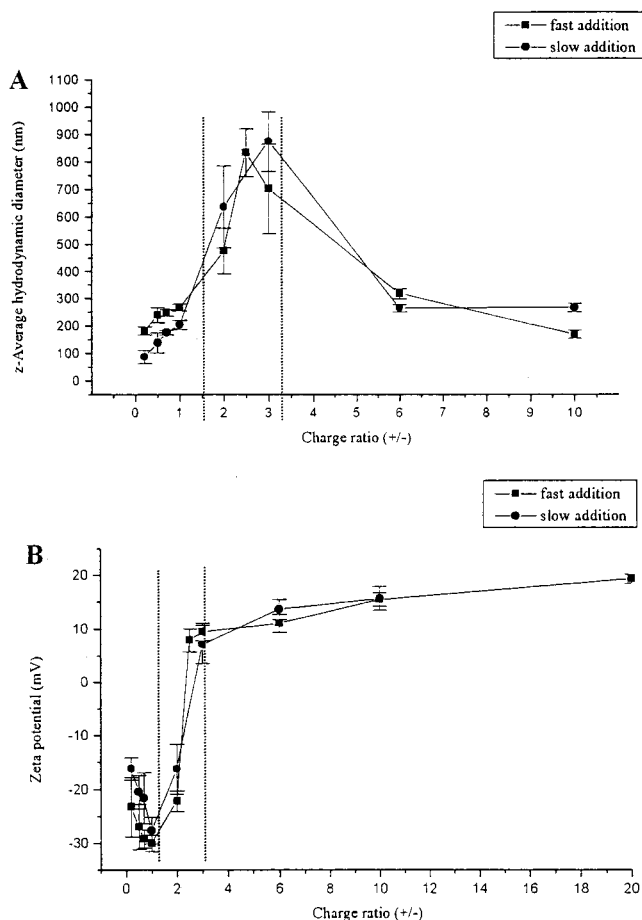


Figure 3. The z-average hydrodynamic diameter (A) and zeta potential (B) of pDMAEMA/Rh-ON complexes, as a function of the charge ratio. The polyplexes were prepared by fast and slow addition of the pDMAEMA solution to the Rh-ON solution, respectively. The Rh-ON concentration in the dispersions was 10 $\mu\text{g}/\text{mL}$. Each measuring point is the mean value of measurements on three dispersions, which were independently prepared. Each dispersion was measured three times.

vidual polyplexes or aggregated polyplexes. As the molecular mass of an individual polyplex can be estimated some hundreds of thousands g/mol (e.g., in case several Rh-ONs bind to 1 pDMAEMA chain), the hydrodynamic diameter must be lower than the values measured in Figure 3, suggesting that aggregated polyplexes are present. As Figure 4A illustrates, aggregation may occur by Rh-ONs, which bridge individual polyplexes. A striking observation in Figure 3A,B is that, at values of $\varphi < 1$, the size of the particles gradually increases, while their ζ gradually decreases, upon adding more pDMAEMA chains. We suggest therefore that increasing pDMAEMA concentration in this region led to more polyplex formation and that aggregation of these polyplexes results in larger structures with lower net negative charge. DLS reveals that fully aggregated polyplexes are formed for values of φ between 1 and 3. For these polyplexes, almost no repulsion occurs between the particles, as ζ approximates zero, which leads to a clustering of individual polyplexes, as presented in Figure 4B.²⁰ Upon further increasing the concentration of pDMAEMA, ζ reaches a positive plateau, indicating a shortage of Rh-ON to compensate the charge. Electrophoresis data prove that at a high value of φ all the Rh-ONs are bound (data not shown). Probably, as illustrated in Figure 4C, as a higher number of pDMAEMA chains are present, the

average number of Rh-ONs bound to one chain is strongly decreased and the nonneutralized cations explains the positive net charge of the polyplexes. The electric repulsion between the positively charged pDMAEMA chains in the polyplexes decreases the size of the pDMAEMA/Rh-ON aggregates at higher φ values (Figure 3A). However, intermolecular bridging of individual polyplexes, as described above, may still occur and explains why the hydrodynamic diameter is much larger than what is expected for individual polyplexes.

An unanswered question is why the interaction between pDMAEMA and Rh-ONs shows a nonstoichiometric behavior, i.e., why ζ crosses over from a negative to a positive value at $\varphi > 1$. Previous studies showed that for many types of cationic polymers ζ crosses over when a the number of positive amino charges on the polymers equals the number of negative phosphate groups on DNA.⁵ Interestingly, upon complexation of salmon sperm DNA instead of ONs to pDMAEMA, ζ crossed over from a negative to a positive value of $\varphi = 1$ (data not shown).

Fluorescence Properties of pDMAEMA/Rh-ON Complexes. Figure 5 shows that, upon complexation of Rh-ON to pDMAEMA, its fluorescence decreases. At values of φ lower than 1, the fluorescence decreases monotonically when the concentration of pDMAEMA increases. The pDMAEMA/Rh-ON complexes having a charge ratio between 2 and 3 show the lowest fluorescence, while at higher φ values their fluorescence again increases. A similar decrease of the fluorescence as seen in Figure 5 was observed in for example the complexation of phosphorothioate ONs to polyamine-poly(ethylene glycol) copolymers and the complexation of fluorescently labeled DNA to polylysine.^{22,23} We hypothesize that the gradual decrease of the fluorescence of the Rh-ONs solutions at low φ values is due to a partial extinction of the fluorescence upon binding of the Rh-ONs to the pDMAEMA chains.

Following the work of Trubetsky et al., who recently reported on the self-quenching of fluorescently labeled DNA upon condensation with polycations, we further investigated whether self-quenching occurs in the pDMAEMA/Rh-ONs polyplexes.²³ Figure 6 shows the fluorescence of pDMAEMA/Rh-ON polyplexes of different charge ratio, prepared by adding the pDMAEMA solution to a mixture of Rh-labeled and nonlabeled ON ("ON + Rh-ON mixture"). While the total ON concentration (10 $\mu\text{g}/\text{mL}$) was fixed, only the percentage of Rh-labeled to unlabeled ON was varied. Three observations can be made from Figure 6. First, at all compositions of the "ON + Rh-ON mixture", adding pDMAEMA decreases the fluorescence of the "ON + Rh-ON mixture". Second, at all φ values, the higher the amount of labeled ONs in the polyplexes, the stronger the fluorescence of the complexes deviates from the fluorescence of the corresponding "ON + Rh-ON mixture" without pDMAEMA. This can only be attributed to self-quenching, which occurs between the Rh-ONs and which becomes more pronounced when more Rh-ONs are present in the complex. Third, the extent of self-quenching as a function of φ , indicated by the slope of the line, increases at low values of φ , is maximal when φ equals 3, and decreases again at high φ values. As illustrated in Figure 4, this has to be explained by a change in the average number of Rh-ONs per complex. At low φ values, by adding more polymer strands to the oligonucleotide solution, self-quenching can occur due

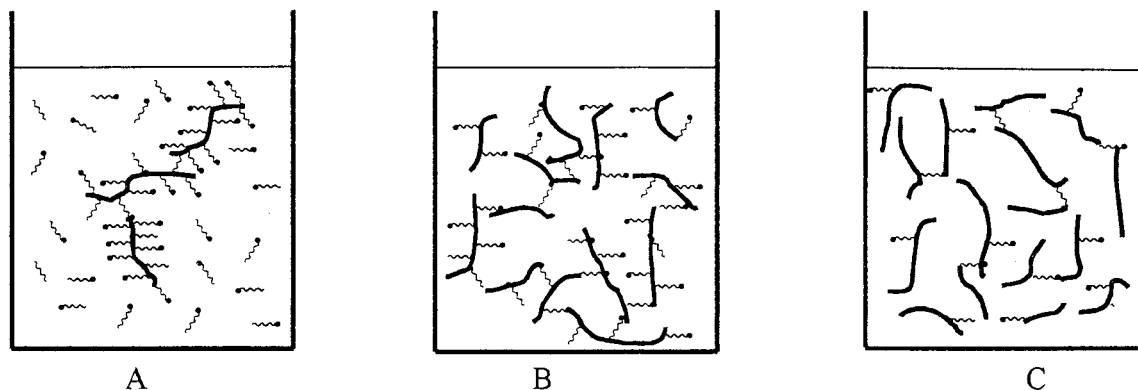


Figure 4. Representation of interactions between Rh-ONs and pDMAEMA under different conditions (A) at low values of φ ($\varphi < 2$), where there is an excess negative charge (B) at intermediates values of φ ($2 < \varphi < 3$) with equal amount of negative and positive charge (C) at high values of φ ($\varphi > 3$) when there is an excess of positive charge.

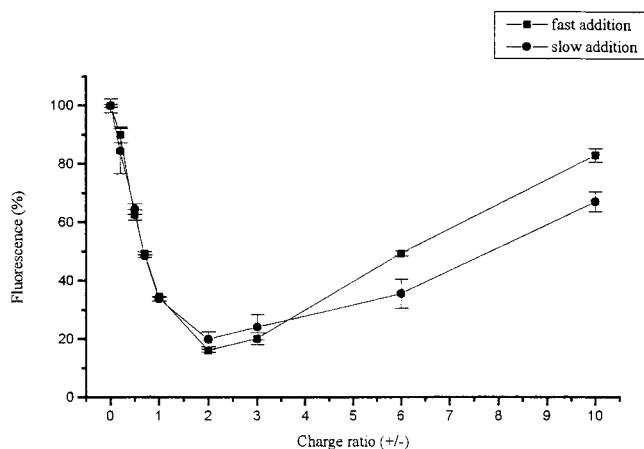


Figure 5. Fluorescence of pDMAEMA/Rh-ON dispersions as a function of the charge ratio. The polyplexes were prepared by fast and slow addition of the pDMAEMA solution to the Rh-ON solution, respectively. The Rh-ON concentration in the dispersions was $10 \mu\text{g/mL}$. The fluorescence of the Rh-ON solution in the absence of pDMAEMA (i.e., at $\varphi = 0$) was set to 100%. Each measuring point is the mean value of measurements on three dispersions, which were independently prepared. Each dispersion was measured three times.

to the formation of multimolecular polyplexes. The Rh molecules come into close proximity of each other and can quench their neighbors. At high φ values, self-quenching decreases as the average amount of Rh-ON per complex probably decreases. For monomolecular complexes, self-quenching would probably not occur as all the Rh-ONs are on different pDMAEMA strands.

Fluorescence Correlation Spectroscopy on Polyplexes. As explained in Materials and Methods, the fluorescence fluctuations, which are monitored in FCS, are caused by the diffusion of the fluorescently labeled molecules through the laser beam. Upon binding of fluorescently labeled molecules (Rh-ONs) to non-fluorescent ones (pDMAEMA), slow fluctuations would have to appear that could be quantified by autocorrelation analysis. Recently, Meseth et al. studied the resolution limit of FCS for two different particles in solution.²⁴ It was shown that, under optimal conditions, the diffusion times should differ by at least a factor of 1.6, which means that the particles must have a molecular weight difference of a factor of 4 assuming the molecular weight to be proportional to D^{-3} . As the molecular mass of the Rh-ONs was 8253 g/mol , while M_n of pDMAEMA was estimated to be $60\,000 \text{ g/mol}$, FCS was evaluated to study the complexation between

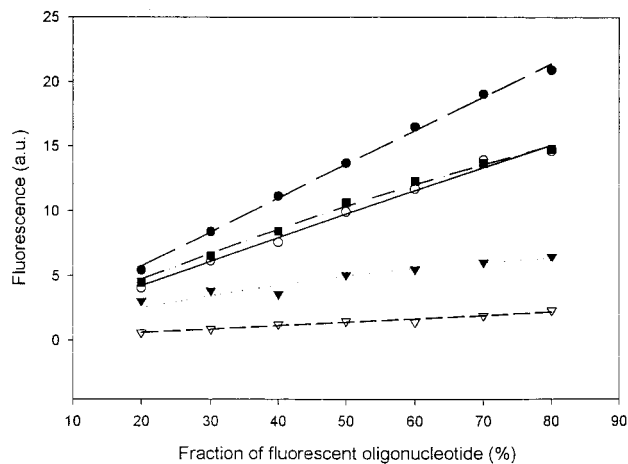


Figure 6. Fluorescence of pDMAEMA/ON + Rh-ON polyplexes prepared by adding (fast addition method) pDMAEMA to "ON + Rh-ON mixtures". The x-axis indicates the percentage of Rh-ON in the "ON + Rh-ON mixtures". $\varphi = 0$ (●) shows the fluorescence of the "ON + Rh-ON mixture" when there was no pDMAEMA present. The values of φ are $\varphi = 0.5$ (○), $\varphi = 1$ (▼), $\varphi = 3$ (▽), and $\varphi = 6$ (■). The ON concentration in the dispersions was $10 \mu\text{g/mL}$.

Rh-ON and pDMAEMA, moreover as FCS shows potential to be applicable in cellular studies.^{25–28}

Rhodamine was preferred as the fluorescent label because, compared to fluorescein, its photophysical characteristics are more suitable for FCS measurements. Fluorescein needs a higher laser light intensity to obtain an acceptable value for the counts per molecule; it is more sensitive to photobleaching and gives rise to a significant triplet state. However, a main disadvantage of Rh is its ability to stick to all types of materials. Especially, as FCS is applied in the nanomolar range of the fluorescent molecules, it is important to take into account this behavior when binding studies are considered. FCS revealed that the storage of Rh-ON solutions in Eppendorf tubes for 10 min decreased the number of molecules in the confocal volume element from 3.9 ± 0.1 to 3.0 ± 0.1 , which coincides with a decrease in concentration from 7.1 to 5.6 nM . The cuvettes used in the FCS measurements did not adsorb Rh-ONs.

Figure 7 shows a compressed representation of the fluorescence fluctuations in the confocal volume (A) and the autocorrelation curve (B) of Rh-ONs in buffer. From the autocorrelation function and the mean diffusion time of the molecules ($193 \pm 4 \mu\text{s}$) a diffusion coefficient

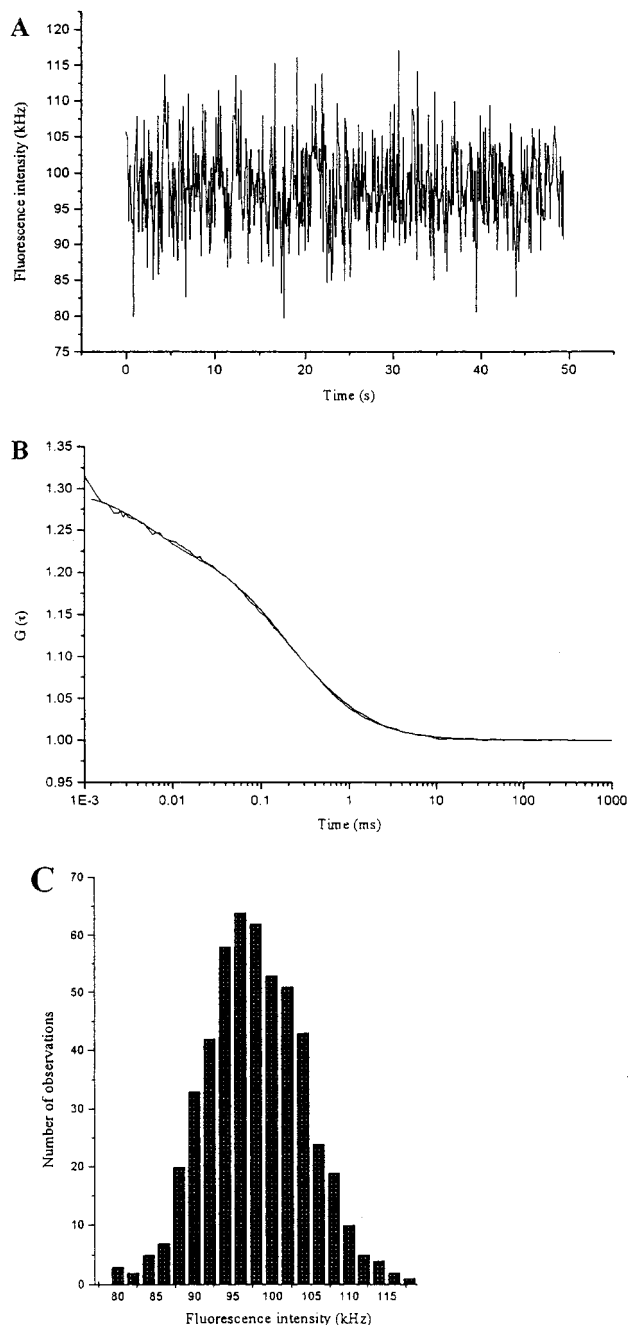


Figure 7. FCS measurements on Rh-ONs in buffer: fluorescence fluctuation profile (A), autocorrelation curve (B), and fluorescence intensity distribution (C). The Rh-ON concentration was $0.025 \mu\text{g/mL}$.

of $1.05 \times 10^{-6} \text{ cm}^2/\text{s}$ was calculated, which agrees with values in the literature. Politz and co-workers measured with FCS a diffusion coefficient of $0.5 \times 10^{-6} \text{ cm}^2/\text{s}$ for a 43-mer ON.²⁸

Figure 8 compares the fluorescence fluctuations of a 3 nM ($0.025 \mu\text{g/mL}$) Rh-ON solution before and after complexation with pDMAEMA. The association of the Rh-ONs with pDMAEMA clearly influences the fluorescence fluctuation profile. First, the fluorescence intensity significantly decreases. Especially, a gradual decrease can be observed when φ of the pDMAEMA/Rh-ON complexes is increased. This agrees with the fluorimetric observations as explained in Figures 5 and 6. Second, highly intense fluorescence peaks became visible upon complexation of Rh-ON to pDMAEMA.

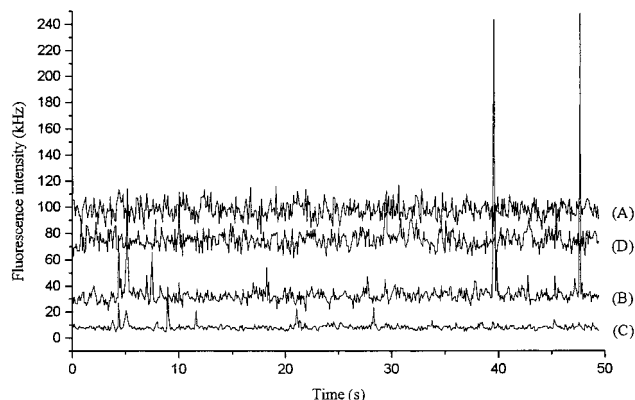


Figure 8. Fluorescence fluctuation profile for respectively a Rh-ON solution (A) and pDMAEMA/Rh-ON dispersions (B: $\varphi = 8$ and 3: $C = 17$). Adding dextran sulfate to the pDMAEMA/Rh-ON dispersions ($\varphi = 17$) partially recovered the fluorescence of the baseline, while the highly intense fluorescence peaks almost disappeared (D). The Rh-ON concentration equaled $0.025 \mu\text{g/mL}$.

Considering the time frame of one measuring point to be 100 ms and the (estimated) diffusion time of polyplexes to be between 1 and 10 ms (see below), one highly intense fluorescence peak does not necessarily originate from the diffusion of one single, very bright polyplex into the confocal volume. It could also be attributed to the diffusion of a number of less bright polyplexes in the confocal volume during the 100 ms time frame.

As multimolecular pDMAEMA polyplexes were revealed from Figure 6, it is highly likely that the highly intense fluorescence peaks originate from the presence of pDMAEMA chains, which bear several Rh-ONs. The heterogeneous distribution of the height of the highly intense fluorescence peaks probably indicates that polyplexes with a polydisperse composition, with regard to the number of Rh-ONs per polyplex, are formed. However, as the discussion above pointed out, the fluorescence of pDMAEMA/Rh-ON complexes may be influenced by many factors; one cannot state that an increase of the height of the highly intense fluorescence peaks by for example factor of 2 is attributed to a doubling of the number of Rh-ONs per complex.

In the measurements of Figure 5, we evaluated to which extent dextran sulfate, an anionic polymer, could destabilize the pDMAEMA/Rh-ON complexes. Upon adding $100 \mu\text{L}$ of a dextran sulfate solution (1 mg/mL in Hepes buffer) to $900 \mu\text{L}$ of pDMAEMA/Rh-ON dispersion ($\varphi = 1$), the fluorescence of the pDMAEMA/Rh-ON dispersion is partially restored (data not shown), which indicates that dextran sulfate competes with the Rh-ONs for binding to pDMAEMA.²⁹ This could also be observed in the FCS data. Figure 8 shows that upon addition of dextran sulfate the fluorescence is partially restored, while the highly intense fluorescence peaks almost disappear.

Although the highly intense fluorescence peaks indicated the presence of the pDMAEMA/Rh-ON complexes (e.g., in Figure 9A), they greatly disturbed the determination of the autocorrelation function from the fluorescence fluctuations (Figure 9B). Especially, using eq 3, it was difficult to calculate the diffusion times and the amount of free and complexed Rh-ON from $G(\tau)$ of the pDMAEMA/Rh-ON dispersions. This forced us to analyze the fluorescence fluctuation profile in an alternative way. For a first approach, we tried to analyze the data by analysis of the photon counting histogram

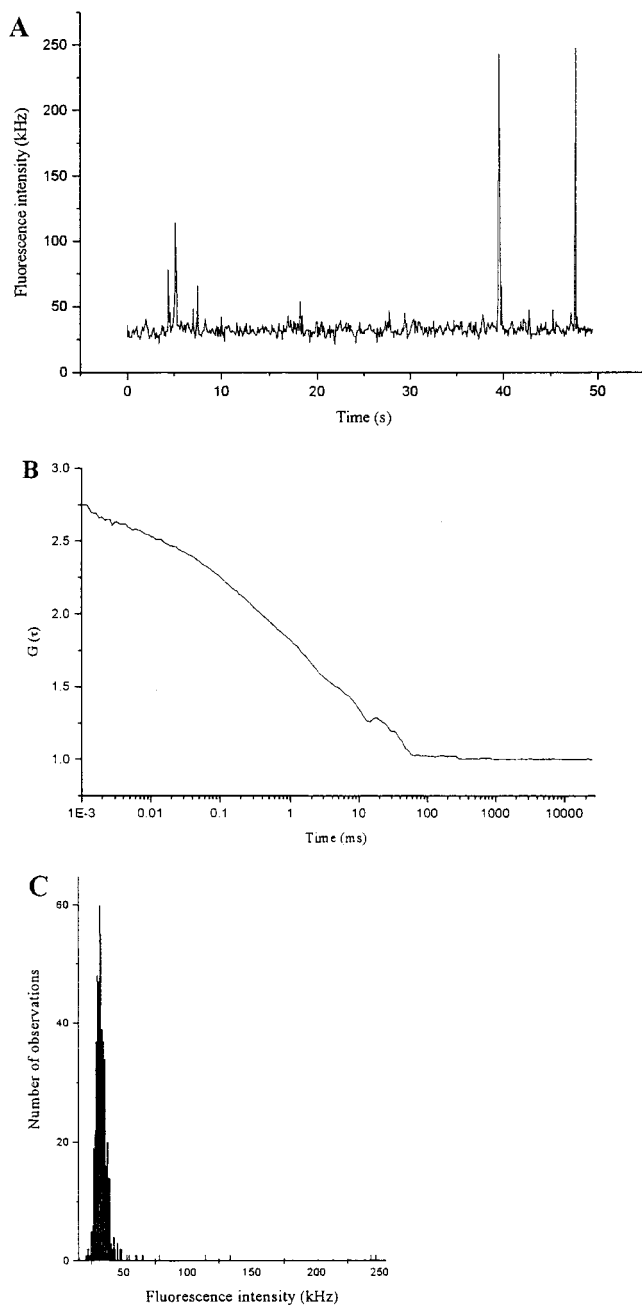


Figure 9. FCS measurements on pDMAEMA/Rh-ON dispersion ($\varphi = 8$): fluorescence fluctuation profile (A), autocorrelation curve (B), and fluorescence intensity distribution (C). The Rh-ON concentration equaled $0.025 \mu\text{g/mL}$.

(PCH) as recently described by Chen and co-workers.³⁰ Due to the “rarity” of the events and the heterogeneity of the formed pDMAEMA/Rh-ON complexes, no appropriate statistics could be done on these data.³²

Recently, a new method was proposed to analyze fluorescence fluctuation profiles of a mixture of different types of fluorescent molecules where one type of the molecules shows much brighter fluorescence with respect to the other, applicable when integration over long time bins has been done.³¹ Van Craenenbroeck et al. performed FCS on mixtures of fluorescein and highly fluorescent 100 nm polystyrene beads. The fluorescence fluctuation profiles, with the appearance of highly intense fluorescence peaks arising from the passage of the fluorescent beads through the confocal volume, resembled the fluorescence fluctuation profiles of pD-

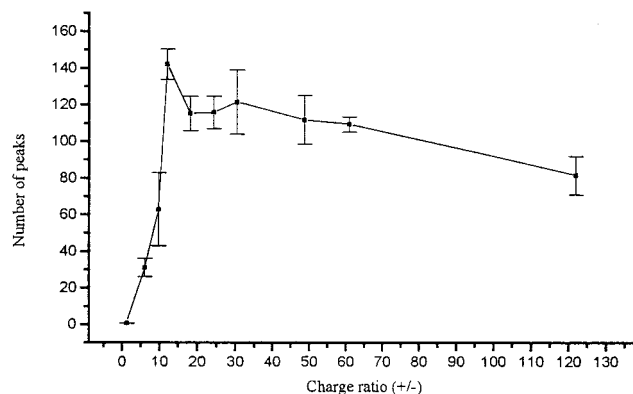


Figure 10. Number of highly intense fluorescence peaks observed in the fluorescence fluctuation profile of pDMAEMA/Rh-ON dispersions as a function of the charge ratio. The Rh-ON concentration equaled $0.025 \mu\text{g/mL}$.

MAEMA/Rh-ON dispersions. They showed that a linear relation exists between the total fluorescence observed in highly intense fluorescence peaks in the fluorescence fluctuation profile and the concentration of the highly fluorescent beads in the mixture. We applied this type of analysis to the fluorescence fluctuation profile of the pDMAEMA/Rh-ON dispersions. When only free Rh-ONs were present, the fluorescence intensities in the fluorescence fluctuation profile (Figure 7A) showed a Gaussian distribution (Figure 7C) with a mean value influenced by the mean number of molecules in the confocal volume and their fluorescence quantum yield, respectively.³¹ The fluorescence fluctuation profile of the pDMAEMA/Rh-ON dispersion showed highly intense fluorescence peaks (Figure 9A) whose intensity did no longer belong to the Gaussian distribution (indicated as “highly intense fluorescence peaks”; Figure 9C). We used the Kolmogorov–Smirnov-based statistical method, as described by Van Craenenbroeck et al.,³¹ to determine above which value of the fluorescence intensities the measured intensities no longer contributed to the Gaussian distribution (“highly intense fluorescence peaks”) and were therefore regarded as originating from pDMAEMA/Rh-ON complexes.³¹ Figure 10 shows the number of the highly intense fluorescence peaks in the fluorescence fluctuation profile of pDMAEMA/Rh-ON complexes. As very low volumes of pDMAEMA solutions were added to the Rh-ON solutions, it was not straightforward to do the FCS measurements at more values of φ between 0 and 10, without using another stock solution. For pDMAEMA/Rh-ON complexes having φ values lower than 15, increasing φ gave rise to an increase in the number of highly intense fluorescence peaks. As the Rh-ON concentration was the same in all the pDMAEMA/Rh-ON dispersions, a higher number of pDMAEMA chains may decrease the average number of Rh-ON bound per pDMAEMA chain as discussed above. This may increase the number of polyplexes which may explain the increase in the number of highly intense fluorescence peaks. However, upon further increasing the number of pDMAEMA chains, one could expect that, from a certain value of φ , polyplexes would arise which consist of only one or a few Rh-ONs bound per pDMAEMA chain and whose fluorescence intensities belong to the Gaussian distribution. Such polyplexes will not result in highly intense fluorescence peaks in the fluorescence fluctuation profile, and consequently it is expected that the number of highly intense fluorescence peaks would decrease.

While it was unclear whether the size, ζ , and fluorimetric data in Figures 3 and 5 concern individual or aggregated polyplexes, due to the use of highly diluted dispersions in FCS, it is highly probable that the diffusion behavior of individual polyplexes is studied in FCS. This can also be observed from the diffusion time, estimated from the time at which G equals the half of $G(0)$, in Figure 9B: the estimated diffusion time is around 1–10 ms. In case clustered polyplexes are present, the diffusion time would probably be much higher. The decrease of the number of RhONs per pDMAEMA chains starts from values of φ around 15 (Figure 10), while this is observed at φ values of 3 in Figure 3A; this might be a consequence of the much lower concentration of the complexes.

Generally, the FCS data could be interpreted on the basis of the properties of the pDMAEMA/Rh-ON complexes as revealed from other methods, although a more quantitative interpretation of the FCS data remains complicated. Especially, the polydispersity of the complexes (both in fluorescence and in molecular size) and the fluorescence quenching upon binding the Rh-ONs to the pDMAEMA chains largely hamper the interpretation of the fluorescence fluctuation profiles.

Summary

DLS, ζ , fluorimetric, and gel electrophoresis experiments, which could be performed when a micromolar Rh-ON concentration (10 $\mu\text{g/mL}$) was used, pointed out that complexation occurs between Rh-ONs and pDMAEMA. In the dependence of size, ζ , and fluorescence of the pDMAEMA/Rh-ON polyplexes on their charge ratio three regions could be clearly distinguished. (1) At values of $\varphi < 1$, only a part of the Rh-ON chains binds to the pDMAEMA chains (as revealed from gel electrophoresis) by a few of their phosphate anions. The nonneutralized anions of the bound ONs provide for the net negative charge of the polyplexes. As the molar mass of an individual polyplex has to be in the order of some hundreds of thousands g/mol and as the hydrodynamic diameters measured on the dispersions ranged from about 80 to 250 nm, it was suggested that aggregation of individual polyplexes occurs by for example Rh-ONs which bridge individual polyplexes. At $\varphi < 1$, the gradual decrease of the fluorescence of the polyplex dispersions upon increasing the amount of pDMAEMA was explained by self-quenching of the fluorescence, as, upon binding, the ONs significantly concentrate. Consequently, the quenching as observed in the fluorescence measurements confirmed the existence of "multimolecular complexes". (2) At values of φ between 1 and 3, DLS revealed that fully aggregated polyplexes were formed. As in this region ζ crosses over from a negative to a positive value and approximates zero, the clustering of the individual polyplexes was attributed to the absence of any repulsion between the particles. (3) At values of $\varphi > 3$, the polyplexes were positively charged, indicating that the polycations in excess incorporated into the complexes. Electrophoresis data indicated that all the Rh-ONs were bound. As in this region the fluorescence of the dispersions again increased it was suggested that, when a higher number of pDMAEMA chains are present, the average number of Rh-ONs bound to one chain begins to decrease, which results in less quenching of the fluorescence. It was suggested that the free cations explain the positive net charge of the polyplexes and that the electric repulsion between the positively charged

pDMAEMA chains on the polyplexes probably decreased the size of the pDMAEMA/Rh-ON complexes.

FCS experiments, which were performed on polyplexes prepared from nanomolar solution of Rh-ONs, also revealed that interactions occur between the Rh-ONs and pDMAEMA. In agreement with the fluorimetric measurements on the micromolar pDMAEMA/Rh-ON dispersions, the fluorescence intensity in the fluorescence fluctuation profiles showed a similar φ dependence. Specifically, highly intense fluorescence peaks appeared in the fluorescence fluctuation profile when complexation between Rh-ON and pDMAEMA occurred. As multimolecular pDMAEMA polyplexes were revealed from fluorimetric measurements on the micromolar pDMAEMA/Rh-ON dispersions, it is very likely that the highly intense fluorescence peaks originated from the presence of pDMAEMA chains which bear several Rh-ONs. For $\varphi < 15$, the number of highly intense fluorescence peaks increased upon adding more pDMAEMA chains to the Rh-ON solution. This was expected as, the more pDMAEMA chains, the more polyplexes and the lower the number of Rh-ONs per polyplex as suggested from the fluorimetric measurements. As expected, from a certain value of φ (around 15) the number of highly intense fluorescence peaks dropped as pDMAEMA/Rh-ON polyplexes arose which probably consist of only one or a few Rh-ONs bound per pDMAEMA.

Acknowledgment. Elke Van Craenenbroeck is a research assistant of FWO-Vlaanderen. The installation of FCS was financially supported by Grant 9.0320.97 from FWO-Vlaanderen, which is acknowledged with gratitude. The Ghent University (UG-BOF) supported this project through instrumentation credits pDMAEMA was synthesized by the group of Professor Dr. W. Hennink (University of Utrecht), who is also acknowledged.

References and Notes

- (1) Cohen, J. S.; Hogan, M. E. *Sci. Am.* **1994**, *271*, 76–82.
- (2) Felgner, P. L.; Barenholz, Y.; Behr, J. P.; Cheng, S. H.; Cullis, P.; Huang, L.; Jessee, J. A.; Seymour, L.; Szoka, F.; Thierry, A. R.; Wagner, E.; Wu, G. *Human Gene Therapy* **1997**, *8*, 511–512.
- (3) Pouton, C. W.; Lucas, P.; Thomas, B. J.; Uduehi, A. N.; Milroy, D. A.; Moss, S. H. *J. Controlled Release* **1998**, *53*, 289–299.
- (4) Mahato, R. I.; Rolland, A.; Tomlinson, E. *Pharm. Res.* **1997**, *14*, 853–859.
- (5) De Smedt, S.; Demeester, J.; Hennink, W. E. *Pharm. Res.* **2000**, *17*, 113–126.
- (6) Kabanov, A. V.; Szoka, F. C.; Seymour, L. W. In *Self-Assembling Complexes for Gene Delivery. From Laboratory to Clinical Trial*; Kabanov, A. V., Felgner, P. L., Seymour, L. W., Eds.; Wiley: New York, 1998; Vol. 10.
- (7) Eastman, S. J.; Siegel, C.; Tousignant, J.; Smith, A. E.; Cheng, S. H.; Scheule, R. K. *Biochim. Biophys. Acta* **1997**, *1325*, 41–62.
- (8) Szoka, F. C. J.; Xu, Y.; Zelphati, O. *J. Liposome Res.* **1996**, *6* (3), 567–587.
- (9) Ottaviani, M. F.; Sacchi, B.; Turro, N. J.; Chen, W.; Jockusch, S.; Tomalia, D. A. *Macromolecules* **1999**, *32*, 2275–2282.
- (10) Wink, T.; de Beer, J.; Hennink, W. E.; Bult, A.; van Bennekom, W. P. *Anal. Chem.* **1999**, *71*, 801–805.
- (11) Cherng, J. Y.; Talsma, H.; Crommelin, D. J. A.; Hennink, W. E. *Pharm. Res.* **1999**, *16*, 1417–1423.
- (12) Cherng, J. Y.; van de Wetering, P.; Talsma, H.; Crommelin, D. J.; Hennink, W. E. *Pharm. Res.* **1996**, *13*, 1038–1042.
- (13) van de Wetering, P.; Zuidam, N. J.; van Steenberg, M. J.; van der Houwen, O. A. G. J.; Underberg, W. J. M.; Hennink, W. E. *Macromolecules* **1998**, *31*, 8063–8068.
- (14) van de Wetering, P.; Cherng, J. Y.; Talsma, H.; Hennink, W. E. *J. Controlled Release* **1997**, *49*, 59–69.

- (15) Cherng, J. Y.; Talsma, H.; Verrijck, R.; Crommelin, D. J.; Hennink, W. E. *Eur. J. Pharm. Biopharm.* **1999**, *47*, 215–224.
- (16) Schwille, P.; Bieschke, J.; Oehlenschläger, F. *Biophys. Chem.* **1997**, *66*, 211–228.
- (17) van de Wetering, P.; Moret, E. E.; Schuurmans, N. N.; van Steenberghe, M. J.; Hennink, W. E. *Bioconjugate Chem.* **1999**, *10*, 589–597.
- (18) Eigen, M.; Rigler, R. *Proc. Natl. Acad. Sci. U.S.A.* **1994**, *91*, 5740–5747.
- (19) Rauer, B.; Neumann, E.; Widengren, J.; Rigler, R. *Biophys. Chem.* **1996**, *58*, 3–12.
- (20) Tang, M. X.; Szoka, F. C. *Gene Ther.* **1997**, *4*, 823–832.
- (21) Trinh, C. K.; Schnabel, W. *Macromol. Chem. Phys.* **1997**, *198*, 1319–1329.
- (22) Vinogradov, S. V.; Bronich, T. K.; Kabanov, A. V. *Bioconjugate Chem.* **1998**, *9*, 805–812.
- (23) Trubetskoy, V. S.; Slattum, P. M.; Hagstrom, J. E.; Wolff, J. A.; Budker, V. G. *Anal. Biochem.* **1999**, *267*, 309–313.
- (24) Meseth, U.; Wohland, T.; Rigler, R.; Vogel, H. *Biophys. J.* **1999**, *76*, 1619–1631.
- (25) Widengren, J.; Rigler, R. *Cell Mol. Biol.* **1998**, *44*, 857–879.
- (26) Brock, R.; Hink, M. A.; Jovin, T. M. *Biophys. J.* **1998**, *75*, 2547–2557.
- (27) Brock, R.; Jovin, T. M. *Cell Mol. Biol.* **1998**, *44*, 847–856.
- (28) Politz, J. C.; Browne, E. S.; Wolf, D. E.; Pederson, T. *Proc. Natl. Acad. Sci. U.S.A.* **1998**, *95*, 6043–6048.
- (29) Dash, P. R.; Toncheva, V.; Schacht, E.; Seymour, L. W. *J. Controlled Release* **1997**, *48*, 269–276.
- (30) Chen, Y.; Muller, J. D.; So, P. T. C.; Gratton, E. *Biophys. J.* **1999**, *77*, 553–567.
- (31) Van Craenenbroeck, E.; Matthys, G.; Beirlant, G.; Engelborghs, Y. *J. Fluoresc.* **1999**, *9*, 325–331.
- (32) Van Rompaey, E.; Chen, Y.; Müller, J. D.; Sanders, N.; Van Craenenbroeck, E.; Engelborghs, Y.; Gratton, E.; De Smedt, S.; Demeester, J. Submitted to *Biol. Chem.*

MA000882M